# Realizing Massive MIMO Effect Using A Single Antenna: A Time-Reversal Approach

Yi Han[†‡], Yan Chen[⋆‡], Beibei Wang[†‡], and K. J. Ray Liu[†‡]

[†] University of Maryland, College Park, MD 20742, USA
[⋆] University of Electronic Science and Technology of China, Chengdu, China
[‡] Origin Wireless Inc., Greenbelt, MD 20770, USA
Email: [†]{yhan1990, bebewang and kjrliu}@umd.edu   [⋆]eecyan@uestc.edu.cn

*Abstract*—**Massive MIMO has shown the great potential in improving the achievable rate with a very large number of antennas. However, several critical challenges in designing the analog front-end and coordinating the large-scale antenna array have to be carefully addressed. Does there exist an alternative that can achieve similar system performance to massive MIMO with a simpler design? In this paper, we show that by using time-reversal approach, with a sufficiently large bandwidth, one can harvest massive multipaths naturally existing in the rich-scattering environment to form a large number of virtual antennas to achieve the desired massive MIMO effect with a single antenna. We analyze the expected achievable rate of the time-reversal system with MMSE waveform. Furthermore, the corresponding asymptotic achievable rate under a massive multipath setting is derived. Experiment result based on real channel measurements shows that, even with only a single antenna, the time-reversal wideband system can achieve comparable performance as the massive MIMO system in terms of expected achievable rate.**

## I. INTRODUCTION

According to the most recent Cisco Visual Networking Index (VNI) annual report [1], the global mobile data traffic grew 74% in 2015. The demand for supporting the fast-growing consumer data rates urges the wireless service providers and researchers to seek a new efficient 5G technology. Massive multiple-input multiple-output (MIMO) is one of "big three" 5G technology [2], which can offer multi-fold benefits such as enormous enhancement in spectral efficiency and power efficiency [3]–[5].

However, several critical challenges must first be addressed. One of the significant challenges is about the analog front-end design, for example, each tiny antenna needs its own power amplifier and ADC. The researchers in Lund University built a 100-antenna MIMO prototype, and the size is $0.8 \times 1.2 \times 1$ m with 300kg weight and 2.5kW average power consumption [6]. Considering the challenges of massive MIMO in arranging and coordinating the large scale antenna array, a natural question to ask is: does there exist a good alternative that can achieve similar system performance to massive MIMO with a simpler implementation? The answer is yes and the time-reversal (TR) signal processing is potentially a counterpart of massive MIMO in 5G communications.

The straightforward approach to realize the massive MIMO effect is through utilizing an excessive amount of physical antennas. On the other hand, it is well known that radio signals will experience many multipaths due to the reflection from various scatters, especially in indoor environment. Through time-reversing the channel response as the waveform, TR can create a focusing effect, which in essence is a spatial-temporal resonance effect that brings the signal on all the multipaths to arrive at a particular location at a specific moment. Such a phenomenon allows us to utilize the naturally existing multipaths as virtual antennas to be an alternative approach to realize massive MIMO effect even with a single antenna. As shown in Fig. 1, TR inherently treats the multipaths in the environment as virtual antennas, similar to MIMO that uses multiple antennas for better spatial multiplexing. In essence, if cooperation of users, e.g. cooperative communications, is a distributed way of achieving MIMO effect of high diversity, then TR is similarly a cooperation of virtual antennas to achieve the massive MIMO effect. The TR waveform is nothing but to control each multipath (virtual antenna) to achieve a desire effect. Of course, what cooperation pays for is the spectral efficiency loss due to the time used for distributed processing, in return for the diversity effect.

TR technique was first introduced to compensate the delay distortion on wired transmission lines [7]. More recently, TR has drawn more attention from researchers in the wireless communications field [8]–[18]. In order to harvest the multipaths, the transmit power and bandwidth can be utilized. Based on the real indoor ultra-wide-band (UWB) channel measurement in [19], around 60-80 independent multipaths can be revealed with a sufficiently large bandwidth. At mmWave band, there still exists a large amount of multipaths indicated by the large delay spread, which is essential for TR communication [20], [21]. Compared with increasing the spectral efficiency, it becomes more important to reduce complexity, total energy consumption and offer other benefits for 5G communication given the potential large bandwidth [2], [22]. Therefore, TR technology is a promising candidate for future communication.

In this paper, we propose a TR technique as an alternative approach to realize massive MIMO effect with much lower complexity. By harvesting the massive multipath in the rich-scattering environment, TR can achieve a similar quasi-orthogonal property of channels in massive MIMO system, which is defined as the TR massive multipath effect. With the massive multipath, the focusing ball of TR will shrink
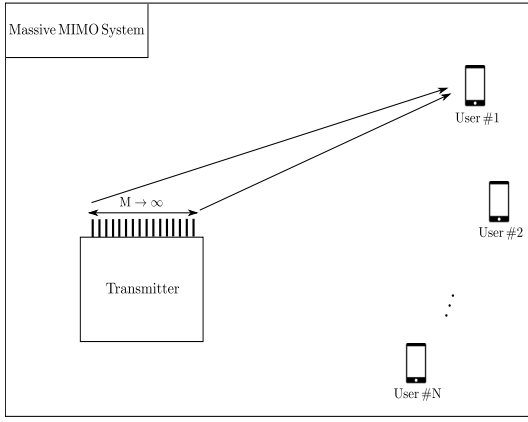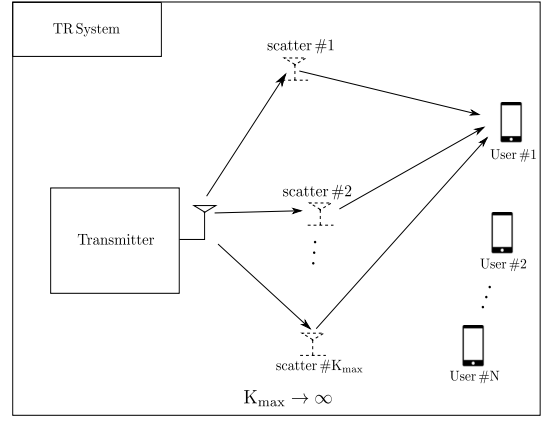
(a) massive MIMO            (b) TR system

Fig. 1.  Comparison between massive MIMO system and TR system

to pinpoint so that two nearby receivers can be supported simultaneously with tiny interference. Through the experiment with real indoor measurements, we show that a TR wideband system can achieve comparable achievable rate as the massive MIMO system with a single antenna.

The rest of this paper is organized as follows. We first discuss the system model in Sec. II. In Sec. III, we demonstrate that a TR Massive Multipath Effect can be achieved in a multipath-rich environment, which is similar to the quasi-orthogonal property of channels in massive MIMO. In Sec. IV, the asymptotic expected achievable rate of the TR system with MMSE waveform is investigated. Experiment results based on real channel measurements are discussed in Sec. V. Finally, Sec. VI concludes the paper.

## II. SYSTEM MODEL

In this paper, we consider a TR downlink system where one transmitter simultaneously communicates with $N$ distinct receivers through the time-reversal division multiple access (TRDMA) technique [11]. We assume that both the transmitter and receivers are equipped with one single antenna.

Suppose there are totally $K_{max}$ independent multipaths from the transmitter to the $j^{th}$ receiver and let $W$ be the bandwidth of the TR system. Then a $L$-tap channel with $L = round(\tau_C W)$ can be resolved for the link between transmitter and the $j^{th}$ receiver as follows

$$\mathbf{h}_j = \Big[ h_{j,1}, \, h_{j,2}, \, \cdots, \, h_{j,L} \Big]^T, \tag{1}$$

where $(\cdot)^T$ stands for transpose operation, $\tau_C$ represents the channel delay spread, $h_{j,i}$ is the complex channel gain of the $i^{th}$ tap, and $h'_{j,i}s$ are independent for all $i \in [1, L]$ and $j \in [1, N]$.

Suppose that there are $K$ non-zero elements in the $L$-tap channel $\mathbf{h}_j$. When the bandwidth $W$ is small, all elements in $\mathbf{h}_j$ are generally non-zero, i.e., $K = L$. On the other hand, when $W$ is sufficiently large, there are at most
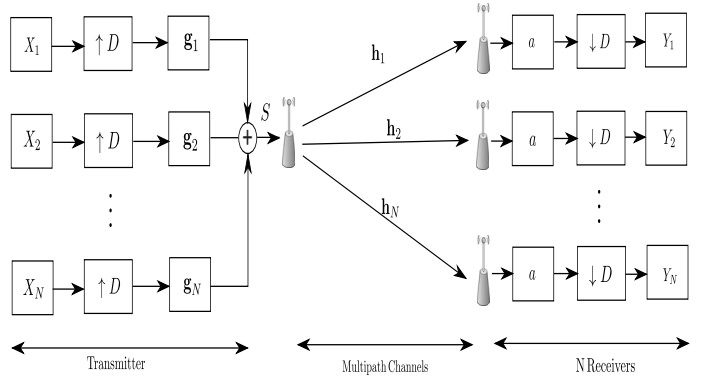
$K = K_{max} < L$ non-zero elements in $\mathbf{h}_j$. Let $\phi_{K_{max}}$ be the non-zero multipath set, which reflects the physical patterns of scatters distribution in the environment. Then, $h_j[k] = 0$ for $k \notin \phi_{K_{max}}$, and for $k \in \phi_{K_{max}}$, $h_j[k]$ is a complex random variable with zero mean and variance $\sigma_k^2$.

The TRDMA system architecture is shown in Fig. 2, where $X_j$ and $\mathbf{g}_j$ represent the information symbol and waveform of the $j^{th}$ receiver. Moreover, $D$ stands for the backoff factor to suppress the ISI. Then, at the receiver side, the $j^{th}$ receiver simply scales the received signal and down-samples it to obtain the estimated signal $Y_j$ as follows

$$Y_j[k] = \mathbf{H}_j^{(\frac{L}{D})}\mathbf{g}_j X_j[k - \frac{L}{D}] + \sum_{l=1, l \neq L/D}^{(2L-1)/D} \mathbf{H}_j^{(l)}\mathbf{g}_j X_j[k - l]$$
$$+ \sum_{l=1}^{(2L-1)/D} \mathbf{H}_j^{(l)} \left( \sum_{i=1, i \neq j}^{N} \mathbf{g}_i X_i[k - l] \right) + n_j[k], \tag{2}$$

where $\mathbf{H}_j^{(m)}$ is the $m^{th}$ row of the $(2L-1)/D \times L$ matrix $\mathbf{H}_j$ decimated by rows of Toeplitz matrix, which can be written



Fig. 2.  TRDMA System

$$\mathbf{H}_j = \begin{pmatrix} h_j[D] & h_j[D-1] & \cdots & h_j[1] & 0 & \cdots & \cdots & 0 \\ h_j[2D] & h_j[2D-1] & \cdots & \cdots & h_j[1] & 0 & \cdots & 0 \\ \vdots & \vdots & \ddots & \ddots & \ddots & \ddots & \ddots & \vdots \\ h_j[L] & h_j[L-1] & \cdots & \cdots & \cdots & \cdots & \cdots & h_j[1] \\ \vdots & \vdots & \ddots & \ddots & \ddots & \ddots & \ddots & \vdots \\ 0 & \cdots & 0 & h_j[L] & \cdots & \cdots & h_j[L-D+1] & h_j[L-2D] \\ 0 & \cdots & \cdots & 0 & h_j[L] & \cdots & h_j[L-D+1] & h_j[L-D] \end{pmatrix}. \tag{3}$$

in (3), and thus $\mathbf{H}_j^{(\frac{L}{D})}$ is the time-reversed channel, i.e.,

$$\mathbf{H}_j^{(\frac{L}{D})} = \left[ h_j[L], \, h_j[L-1], \cdots, h_j[1] \right]. \tag{4}$$

### III. TR Massive Multipath Effect

Similar to the quasi-orthogonal property in massive MIMO given an excessive amount of antennas [5], the multipath profile of different users in the TR system will also be orthogonalized given massive independent multipaths, which we call the TR Massive Multipath Effect (TRMME).

**Theorem 1 (Time-Reversal Massive Multipath Effect):** When $K_{max}$ is sufficiently large, with the asymptotic setting that $W \to \infty$ to resolve all the multipaths, we have

$$\begin{cases} [\mathbf{QQ}^\dagger]_{m,n} & \xrightarrow{d} 0, \; \text{if } m \neq n \\ \dfrac{[\mathbf{QQ}^\dagger]_{m,m}}{\lambda_m} & \xrightarrow{d} 1, \; \text{otherwise} \end{cases}, \tag{5}$$

where $\mathbf{Q} = [\mathbf{H}_1^T, \mathbf{H}_2^T, \cdots, \mathbf{H}_N^T]^T$, $\xrightarrow{d}$ represents the convergence in distribution, and $\lambda_m = \|\mathbf{h}_j\|^2$ if $m = (j-1)(2L-1)/D + L/D$.

*Proof.* In a massive multipath environment, $K_{max}$ is sufficiently large but finite. To reveal all the multipaths, we consider the asymptotic setting that $W \to \infty$. Notice that every element in $\mathbf{QQ}^\dagger$ is the sum of multiple independent variables, which converges to a Gaussian random variable in distribution in the asymptotical scenario based on the central limit theorem. Since Gaussian random variable is only determined by the first and second moment and obviously each element in $\mathbf{QQ}^\dagger$ has zero mean, we only need to prove the largest variance of the off-diagonal elements will converge to zero.

Based on the definition of $\mathbf{Q}$, we can directly obtain

$$\left[\mathbf{QQ}^\dagger\right]_{l_j, l_j} = \mathbf{H}_j^{(\frac{L}{D})} \mathbf{H}_j^{(\frac{L}{D})\dagger} = \|\mathbf{h}_j\|^2, \tag{6}$$

where $[\cdot]_{m,n}$ represents the element in the $m^{th}$ row and the $n^{th}$ column of the matrix.

Then, we prove that $\mathbf{QQ}^\dagger$ is diagonal by examining the off-diagonal elements. Considering each off-diagonal matrix $\mathbf{H}_i \mathbf{H}_j^\dagger$ ($\forall i \neq j$), we can see that each element of $\mathbf{H}_i \mathbf{H}_j^\dagger$, $\left[\mathbf{H}_i \mathbf{H}_j^\dagger\right]_{m,n} = \mathbf{H}_i^{(m)} \mathbf{H}_j^{(n)\dagger}$, is the sum of multiple independent random variables. Therefore, when $K_{max}$ is sufficiently large, $\left[\mathbf{H}_i \mathbf{H}_j^\dagger\right]_{m,n}$ can be regarded as a Gaussian random variable, whose distribution is completely determined by the first and the second moment.

Based on the independence among the channel taps and distinct receivers, it is obvious that $\mathbf{H}_i^{(m)} \mathbf{H}_j^{(n)\dagger}$ has zero mean. While the second moment can be upper bounded as

$$\mathbb{E}\left[|\mathbf{H}_i^{(m)} \mathbf{H}_j^{(n)\dagger}|^2\right] \leq \left(\sum_{k=1}^{K_{max}} \sigma_k^2\right)^2 / L, \tag{7}$$

which comes from the fact that the $K_{max}$ multipaths are randomly distributed in the $L$-tap channel and thus

$$\mathbb{E}\left[|h_j(m)|^2\right] = \mathbb{E}\left[|h_j(n)|^2\right] = \sum_{k=1}^{K_{max}} \sigma_k^2 / L, \quad \forall m, n. \tag{8}$$

Due to the path loss attenuation, $\sigma_k^2 \leq 1$, which means that $\sum_{k=1}^{K_{max}} \sigma_k^2 \leq K_{max}$. Under the asymptotic setting that $W \to \infty$, $L \to \infty$ according to the definition that $L = round(\tau_C W)$. Since $K_{max}$ is finite, $K_{max}^2/L \to 0$ as $W \to \infty$, i.e., (8) goes to 0. Based on zero mean and (7), we can conclude that

$$\lim_{W \to \infty} \left[\mathbf{H}_i \mathbf{H}_j^\dagger\right]_{m,n} = 0, \quad \forall m, n, \text{ and } i \neq j. \tag{9}$$

Next, let us examine the diagonal submatrix $\mathbf{H}_j \mathbf{H}_j^\dagger$ of $\mathbf{QQ}^\dagger$. Similarly, each element $\left[\mathbf{H}_j \mathbf{H}_j^\dagger\right]_{m,n} = \mathbf{H}_j^{(m)} \mathbf{H}_j^{(n)\dagger}$ can be regarded as a Gaussian variable when $K_{max}$ is sufficiently large. Since $\mathbf{H}_j^{(m)}$ and $\mathbf{H}_j^{(n)}$ are independent when $m \neq n$, similarly we can derive

$$\begin{cases} \mathbb{E}\left[\mathbf{H}_j^{(m)} \mathbf{H}_j^{(n)\dagger}\right] & = 0, \quad m \neq n, \\ \mathbb{E}\left[|\mathbf{H}_j^{(m)} \mathbf{H}_j^{(n)\dagger}|^2\right] & \leq \dfrac{(\sum_{k=1}^{K_{max}} \sigma_k^2)^2}{L}, \quad m \neq n, \end{cases} \tag{10}$$

and given $K_{max}^2/L \to 0$ as $W \to \infty$, we derive that

$$\lim_{W \to \infty} \left[\mathbf{H}_j \mathbf{H}_j^\dagger\right]_{m,n} = 0, \quad \forall j, \text{ and } m \neq n. \tag{11}$$

Therefore, we can conclude that $\mathbf{QQ}^\dagger$ is diagonal. This completes the proof. $\square$

Based on the indoor measurements with the TR prototype in [17], TR with a 125MHz bandwidth is capable to create a spatial focusing ball as shown in Fig. 3. With the derived TRMME, the focusing ball of TR naturally shrinks to a pinpoint in a rich-scattering environment with a sufficiently large bandwidth, which is also predicted and observed in the massive MIMO system [4]. Therefore, the derived TRMME is a counterpart of the massive MIMO effect in indoor scenarios.

In practice, we only need that $K_{max}$ is large enough to achieve massive multipath effect. Based on the real indoor measurement with channel sounder, we notice that the number of the resolved multipaths in a typical indoor environment is
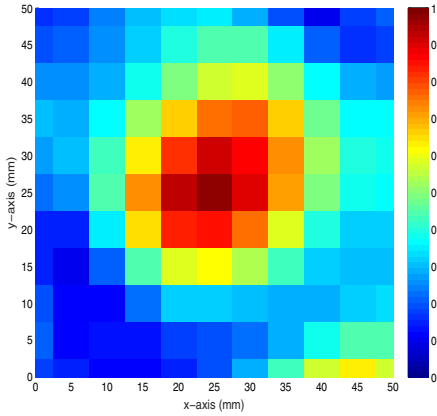
Fig. 3. Spatial Focusing Ball with 125MHz Bandwidth



Fig. 4. Asymptotic performance with $D = K_{max}$, $N = 6$ and $p_u = 5$dB.

large enough (around 100) given a sufficiently large bandwidth.

## IV. ASYMPTOTIC EXPECTED ACHIEVABLE RATE

In this section, we analyze the asymptotic expected achievable rate of the TR system with MMSE waveform [13], i.e.,

$$\mathbf{g}_j = c_{MMSE}\left(\mathbf{Q}^\dagger\mathbf{Q} + \frac{1}{p_u}\mathbf{I}\right)^{-1}\mathbf{Q}^\dagger\mathbf{e}_{l_j}, \qquad (12)$$

where $c_{MMSE}$ is normalization constant, $\mathbf{e}_{l_j}$ is an elementary vector, $\mathbf{I}$ is the identity matrix, and $p_u$ is the transmitting signal-to-noise ratio (SNR) of each user that equals to $P/NP_n$, where $P$ is the transmit power, $P_n$ is the noise power and $N$ is the number of receivers. Note that (12) is derived under the uniform power allocation in the dual uplink and thus has a simple closed form.

By substituting (12) into the expected achievable rate derived from (2) in its dual uplink format [23], the expected achievable rate of the TR system with MMSE waveform can be written as follows,

$$R_j^{MMSE} = \frac{W}{D}\mathbb{E}\left[\log_2\left(\frac{1}{\left[(\mathbf{I} + p_u\mathbf{Q}\mathbf{Q}^\dagger)^{-1}\right]_{l_j,l_j}}\right)\right]. \qquad (13)$$

When $K_{max}$ is sufficiently large, the asymptotic expected achievable rate under $W \to \infty$, the asymptotic expected achievable rate can be derived based on (13) and Theorem 1, which satisfies that

$$\lim_{W\to\infty} \frac{R_j^{MMSE}}{W/D} = \mathbb{E}\left[\log_2\left(1 + p_u\|\mathbf{h}_j\|^2\right)\right]. \qquad (14)$$

From (14), the TR system achieves the optimal AWGN rate, where the ISI and IUI are completely cancelled out with the beamforming on virtual antennas in the multipath-rich environment.
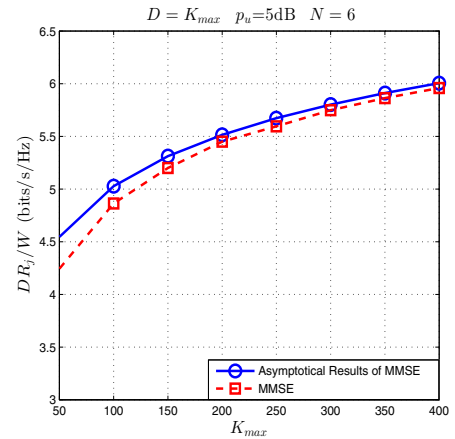
## V. SIMULATIONS AND EXPERIMENTS

In this section, we conduct simulations and experiments to evaluate the expected asymptotical performance of a TR system. We assume that the $N$ receivers are uniformly, randomly distributed and share the same channel model with the expected channel gain as an increasing function of the number of independent multipaths.

### A. Asymptotical Performance

We first validate our theoretical analysis in (14). The expected performance of each receiver is shown in Fig. 4 with $p_u = 5$dB and $N = 6$. The y-axis is $DR_j/W$, where $R_j$ is the expected achievable rate of the $j^{th}$ receiver, $D$ is the backoff factor and $W$ is the system bandwidth. From Fig. 4, we can observe that the expected asymptotical performance using MMSE waveform converges to (14) quickly as $K_{max}$ increases.

### B. The Number of Observable Independent Multipaths in A Typical Indoor Environment

Achieving the asymptotic performance in (14) requires the TR system to operate in a multipath-rich environment. In this subsection, we investigate the number of observable independent multipaths $K$ in a typical indoor environment using real-world measurements. We demonstrate that, in a typical office, the number of resolvable multipaths is large with a sufficiently large bandwidth.

We use two Universal Software Radio Peripherals (USRPs) as channel sounders to probe the channel in a typical office room, whose floor plan is shown in Fig. 5. As shown in the figure, the TX is placed on a grid structure with 5cm resolution and the RX is placed at the corner. With two USRPs, we scan the spectrum, e.g., from 4.9GHz to 5.9GHz, to acquire the channel impulse responses with a bandwidth of 10MHz-1GHz.

We employ eigenvalue analysis to determine the value of $K$ for any given bandwidth $W$. First, we estimate the covariance
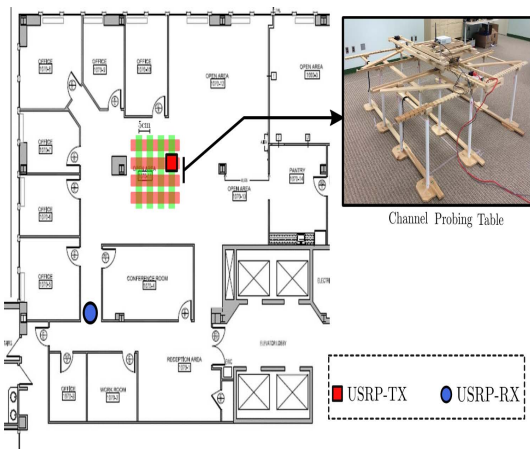
Fig. 5.   Floor Plan and Experiment Setting
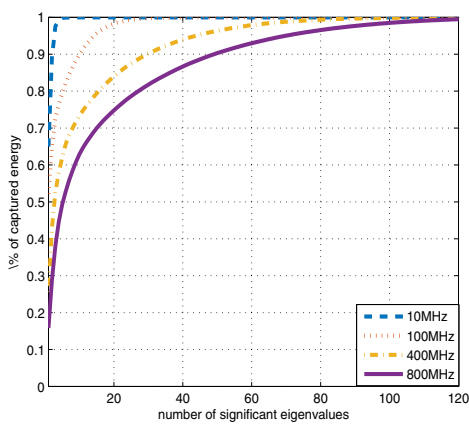


Fig. 7.   Number of significant eigenvalues $K$ at different bandwidth $W$.

degree of freedom $K$ increases as the bandwidth $W$ increases. This is further confirmed in Fig. 7, where we show the number of significant eigenvalues versus the channel bandwidth by fixing the captured energy at 98%.

### C. Comparison with Massive MIMO

In this subsection, we evaluate the expected achievable rate of the TR system based on (13) using the real channel measurements from channel sounder in a typical office, with $W = 1$GHz. From the measurements, around 100 independent multipaths can be resolved through eigenvalue analysis as shown in Fig. 7. Then we compare the performance of the TR system with that of a massive MIMO system.

We choose $D = 30$ as the backoff factor used in a TR system and compare the expected achievable rates using MMSE waveforms to that of a genie-aided massive MIMO system, where "genie-aided" means the interference, antenna coupling effects and the loss due to cyclic prefix are ignored. Assume the genie-aided massive MIMO system has a bandwidth $W_{MM}$ and $M$ antennas at the transmitter [3], then the user $j$'s expected achievable rate can be calculated as $\mathbf{R}_j^{MM} = W_{MM}\mathbb{E}\left[\log_2\left(1 + p_u\|\widehat{\mathbf{h}}_j\|^2\right)\right]$, where $W_{MM}$ is chosen as 20MHz according to the massive MIMO prototype [6].

It is shown in Fig. 8 that TR system can achieve comparable achievable rate as that of massive MIMO system in practical indoor environment. Note that TR method pays the price of spectral efficiency loss for the low cost and complexity implementation for indoor communications. For example, as shown in Fig. 9 [17], the TR prototype is a customized software defined radio (SDR) platform for designing and deploying TR-based communication systems. The size of the radio is 5cm by 17cm by 23cm, the weight is about 400g, and the power consumption is 25W. Compared with the massive MIMO prototype built in [6], the complexity and operation power consumption are obviously much lower. Considering the potential wide bandwidth available in future (e.g., UWB and mmWave band), the complexity, energy consumption and



Fig. 6.   Percentage of captured energy versus the number of significant eigenvalues with a single antenna

matrix of the measured channels $\mathbf{K}_{h,W}$ using the statistical averaging, i.e.,

$$\mathbf{K}_{h,W} = \frac{1}{N}\sum_{i=1}^{N}\mathbf{h}_{i,W}\mathbf{h}_{i,W}^{\dagger}, \tag{15}$$

where $\mathbf{h}_{i,W}$ is the channel information obtained at the location $i$ with the bandwidth $W$ and $N = 100$. Since $\mathbf{K}_{h,W}$ is Hermitian and positive definite, there exists a unitary matrix $U$ such that

$$\mathbf{K}_{h,W} = U\Lambda U^{\dagger} = \sum_{i=1}^{L}\lambda_{i,W}\psi_i\psi_i^{\dagger}, \tag{16}$$

where $\lambda_{1,W} \geq \lambda_{2,W} \geq \cdots \geq \lambda_{L,W}$ and $L = \tau_C W$.

In Fig. 6, we show the percentage of the captured energy $E_l$ versus the number of significant eigenvalues $l$, with $E_l$ defined as $E_l = \frac{\sum_{i=1}^{l}\lambda_i}{\sum_{i=1}^{L}\lambda_i}$. From Fig. 6, we can see that the channel energy is concentrated in a small number of eigenvalues when the bandwidth is small, while spread over a large number of eigenvalues as the bandwidth increases. In other words, the
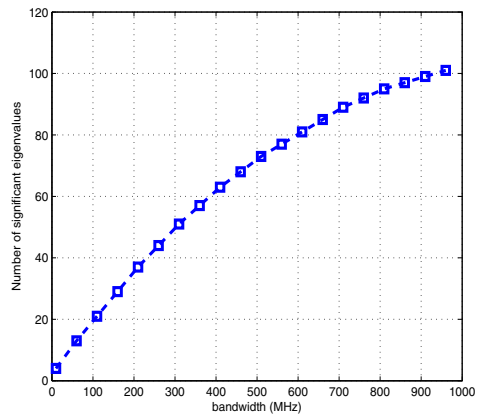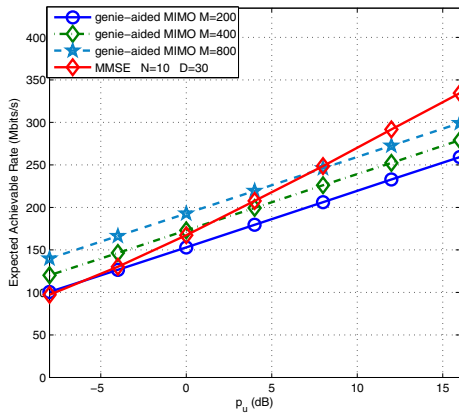
Fig. 8. Expected achievable rate comparison between TR and massive MIMO systems, with $W = 1GHz$, $N = 10$ and $D = 30$ for the TR system, and $W_{MM} = 20MHz$.
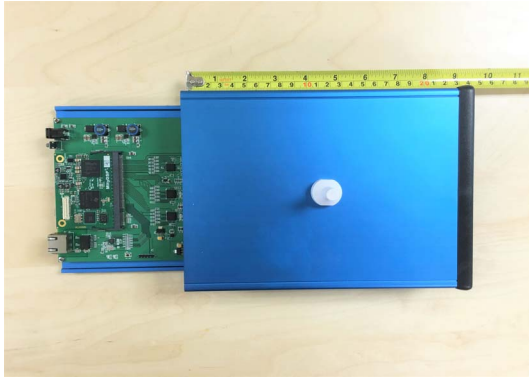


Fig. 9. TR prototype

other metrics become more and more important compared with the spectral efficiency in indoor scenarios, which makes the TR technology a promising candidate for indoor communication.

## VI. CONCLUSION

In this paper, we demonstrate that the TR can harvest naturally existing multipaths as virtual antennas, when given a large enough bandwidth, to offer a cost effective solution to achieve massive MIMO effect. We also show in real experiments that the TRMME can obtain similar achievable rate as that of massive MIMO system using hundreds of real antennas. When ADC technology advances, the larger bandwidth is getting more affordable, especially at UWB band or at the higher frequency range such as mmWave. TR offers an excellent alternative to realize massive MIMO effect for 5G systems, especially for indoors or environments with a large number of multipaths. On the contrary, the straightforward realization of massive MIMO by using hundreds of antennas may continue to face the challenge in the hardware design.

## REFERENCES

[1] Cisco, "Visual networking index," *Cisco white paper*, 2016.

[2] J.G. Andrews, S. Buzzi, Choi Wan, S.V. Hanly, A. Lozano, A.C.K. Soong, and J.C. Zhang, "What will 5g be?," *IEEE J. Sel. Areas Commun.*, vol. 32, no. 6, pp. 1065–1082, 2014.

[3] H.Q. Ngo, E.G. Larsson, and T.L. Marzetta, "Energy and spectral efficiency of very large multiuser mimo systems," *IEEE Trans. Commun.*, vol. 61, no. 4, pp. 1436–1449, 2013.

[4] F. Rusek, D. Persson, B.K. Lau, E.G. Larsson, T.L. Marzetta, O. Edfors, and F. Tufvesson, "Scaling up mimo: opportunities and challenges with very large arrays," *IEEE Signal Proces. Mag.*, vol. 30, no. 1, pp. 40–46, 2013.

[5] T.L. Marzetta, "Noncooperative cellular wireless with unlimited numbers of base station antennas," *IEEE Trans. Wireless Commun.*, vol. 9, no. 11, pp. 3590–3600, 2010.

[6] J. Vieira, S. Malkowsky, K. Nieman, Z. Miers, N. Kundargi, Liang Liu, I. Wong, V. Owall, O. Edfors, and F. Tufvesson, "A flexible 100-antenna testbed for massive mimo," *in Proc. IEEE GC Wkshps*, pp. 287–293, 2014.

[7] B. P. Bogert, "Demonstration of delay distortion correction by time-reversal techniques," *IRE Trans. Commun. Syst.*, vol. 5, no. 3, pp. 2–7, 1957.

[8] H.T. Nguyen, J.B. Anderson, and G.F. Pedersen, "The potential of time reversal techniques in multiple element antenna systems," *IEEE Commun. Lett.*, vol. 9, no. 1, pp. 40–42, 2005.

[9] B. Wang, Y. Wu, F. Han, Y.H. Yang, and K. J. Ray Liu, "Green wireless communications: a time-reversal paradigm," *IEEE J. Select. Areas Commun.*, vol. 29, no. 8, pp. 1698–1710, 2011.

[10] M.-A. Bouzigues, I. Siaud, M. Helard, and A.-M. Ulmer-Moll, "Turn back the clock: time reversal for green radio communications," *IEEE Veh. Technol. Magazine*, vol. 8, no. 1, pp. 49–56, 2013.

[11] F. Han, Y.H. Yang, B. Wang, Y. Wu, and K. J. Ray Liu, "Time-reversal division multiple access over multi-path channels," *IEEE Trans. Commun.*, vol. 60, no. 7, pp. 1953–1965, 2012.

[12] Y. Jin, J. Yi, and J.M.F. Moura, "Multiple antenna time reversal transmission in ultra-wideband communications," *in Proc. IEEE GlOBECOM*, pp. 26–30, 2007.

[13] Yu-Han Yang, Beibei Wang, W Sabrina Lin, and K. J. Ray Liu, "Near-optimal waveform design for sum rate optimization in time-reversal multiuser downlink systems," *IEEE Trans. Wireless Commun.*, vol. 12, no. 1, pp. 346–357, 2013.

[14] E. Yoon, S. Kim, and U. Yun, "A time-reversal-based transmission using predistortion for intersymbol interference alignment," *IEEE Trans. Commun.*, vol. 63, no. 2, pp. 455–465, 2014.

[15] Yan Chen, Yu-Han Yang, Feng Han, and K. J. Ray Liu, "Time-reversal wideband communications," *IEEE Signal Process. Lett.*, vol. 20, no. 12, pp. 1219–1222, 2013.

[16] Y. Chen, F. Han, Y.H. Yang, H. Ma, Y. Han, C.X. Jiang, H.Q. Lai, D. Claffey, Z. Safar, and K. J. Ray Liu, "Time-reversal wireless paradigm for green internet of things: an overview," *IEEE Internet Things J.*, vol. 1, no. 1, pp. 81–98, 2014.

[17] Zhung-Han Wu, Yi Han, Yan Chen, and K. J. R. Liu, "A time-reversal paradigm for indoor positioning system," *IEEE Trans. Veh. Technol.*, vol. 64, no. 4, pp. 1331–1339, 2015.

[18] R. de Lacerda, L. Cottatellucci, A. Hayar, and M. Debbah, "Asymptotic analysis of channel division multiple access schemes for ultra-wideband systems," *in Proc. IEEE SPAWC*, pp. 186–190, 2008.

[19] R. Saadane, A. Menouni, R. Knopp, and D. Aboutajdine, "Empirical eigenanalysis of indoor uwb propagation channels," *in Proc. IEEE GLOBECOM*, vol. 5, pp. 3215–3219, 2004.

[20] T.S. Rappaport, Shu Sun, R. Mayzus, Hang Zhao, Y. Azar, K. Wang, G.N. Wong, J.K. Schulz, M. Samimi, and F. Gutierrez, "Millimeter wave mobile communications for 5g cellular: It will work!," *IEEE Access*, vol. 1, pp. 335–349, 2013.

[21] G. R. Maccartney, T. S. Rappaport, S. Sun, and S. Deng, "Indoor office wideband millimeter-wave propagation measurements and channel models at 28 and 73 ghz for ultra-dense 5g wireless networks," *IEEE Access*, vol. 3, pp. 2388–2424, 2015.

[22] C. X. Wang, F. Haider, X. Gao, X. H. You, Y. Yang, D. Yuan, H. M. Aggoune, H. Haas, S. Fletcher, and E. Hepsaydir, "Cellular architecture and key technologies for 5g wireless communication networks," *IEEE Communications Magazine*, vol. 52, no. 2, pp. 122–130, February 2014.

[23] D. Tse and P. Viswanath, "Downlink-uplink duality and effective bandwidths," *in Proc. IEEE ISIT*, 2002.